A new method to quantify mineral textures for geometallurgy

Cecilia Lund[a*], Pertti Lamberg[a] and Therese Lindberg[b]

[a] MiMeR – Minerals and Metallurgical Research Laboratory, Luleå University of Technology, 971 87 Luleå, Sweden
[b] LKAB, Research & Development, 983 81 Malmberget, Sweden

* Corresponding author. Tel.: +46 920 492354. E-mail address: cecilia.lund@ltu.se

Key words

Geometallurgical model, iron ore, mineral textures, Particle Tracking, textural archetypes

Abstract

A geometallurgical model was developed in three steps using the Malmberget iron ore deposit, northern Sweden as a case study. It is based on a mineralogical-particle approach which means that the mineral information is in the focus. Firstly, the geological model describes quantitatively the variation within the ore body in modal composition and mineral textures. Traditional geological textural descriptions are qualitative and too vague and therefore a method that describes and distinguishes quantitatively different mineral textures and creates different types called textural archetypes was developed.

The second part of the geometallurgical model is a sub-model which forecasts how ore will break and which kind of particles will be generated. A simple algorithm was developed to estimate the liberation distribution for the progenies of each textural archetype. The model enables numerical prediction of the liberation spectrum with varying modal mineralogy. The third step includes a process model describing quantitatively how different particles behave in each unit process stage. As a whole the geometallurgical model takes the spatial information of the geological model in terms of modal composition and textural type. The particle breakage model forecasts the liberation distribution of the corresponding feed to the concentration process and the process model returns the metallurgical response in terms of product quality (grade) and effectively (recovery).

1 Introduction

The geometallurgy embraces geological and metallurgical information to create spatially-based predictive model (3D) for mineral processes (Lamberg, 2011). The industrial application is called geometallurgical program which is a structured effort to bridge all the adherent knowledge of the resource for production planning and management.

Geometallurgical programs are needed for better resource management and to lower the risk in the process operation related to geological variations within the ore body. It is a vital part of the profitability of the operation. The mine needs to be capable to adjust the concentration process and the product qualities to meet the requirements of a changeable global marked e.g. by a more effective utilisation of the ore resources or handle larger volumes of lower grade ore. Today there exist different kinds of geometallurgical models depending on the ore, its quality and the mineral processing circuit (Alruiz et al., 2009; Suazo et al., 2010; Hunt et al., 2012).

Most of the geometallurgical programs are established by using certain steps and relies on metallurgical and geometallurgical testing (Dobby et al., 2004; Bulled and McInnes, 2005; David, 2007; Lamberg, 2011). A series of representative ore samples are collected and are then tested to measure the metallurgical response directly with a standard methodology (e.g. standard flotation test). There are high expectations on the representativeness of the samples and tests since they link the ore and metallurgical response. As the sample set should include all variability in the ore this is often called a variability test. Based on the test results, a mathematical model is created to explain the metallurgical response based on the sample characteristics. The model parameters are almost always chemical components not minerals.

Iron mines are big volume operations and the production is driven by throughput. Lots of the mining companies produce high volumes of relatively low grade iron ore products with a Fe grade between 62% and 64%. Examples of such production are direct shipping of hematite ores in Australia and Brazil. The LKAB, Swedish iron ore producer, represents totally another end of production strategy. They produce customer tailored high grade iron ore pellets (>67% Fe) and fines for blast furnaces and direct reduction (LKAB, 2011).

Good understanding on the raw material and its variability are essential in both the strategies. In the direct shipping ores the production chain is very short; normally it includes only crushing and screening, and therefore if the ore is not suitable for the product requirements the tools in mineral processing are very few. In the high grade products; where the tolerable grade of impurities like silica, aluminium, phosphorous and sulphur, are very low; the success of processing is very dependent on the ore quality and its identification before it comes to the plant.

In the literature there is very little information on the existing geometallurgical programs of iron ores, but a few can be found, i.e. from Kiruna, Sweden (Niiranen and Böhm, 2012) and NW Australia (Paine et al., 2011). Technique that is frequently used in evaluating the metallurgical variation in magnetite bearing iron ores is Davis tube (Farrell et al., 2011; Niiranen and Böhm, 2012). It is a small scale magnetic separation test and the ore samples are normally ground to the liberation size before testing. The corresponding concentrate and tail are chemically analysed and the distribution of elements is then calculated. The iron distribution (recovery) and the concentrate quality are used in predicting the metallurgical response in full scale operation.

The problem with using only the chemical components is that they are not the primary neither the direct reason for the metallurgical response. As chemical components are bond in minerals it is more appropriate to use mineralogy for building the metallurgical functions and the geometallurgical domains. However, minerals do not occur independently in the processes they occur in particles which is varying in size, shape and composition.

Lund et al. (2013) developed a practical, fast and inexpensive method to derive modal composition from routine chemical assays using an element to mineral conversion technique which formed the first part of a geometallurgical model of the Malmberget deposit. However, the modal mineralogy is not sufficient to solely answer the ore behaviour when processing the ore. The mineral textures play a significant role and need to be considered when a geometallurgical model is developed.

The texture characterisations are usually very subjective (Bonnici et al., 2008) and traditionally more related to ore characterisation than process mineralogy (Perez-Barnuevo et al., 2012). In a mineral process, the mineral textures and the liberation are closely associated. The included textures are one important parameter that determines the limitation in an upgrading process (Butcher, 2010). The purpose of the comminution stage is to liberate ore minerals appropriately for the concentration process to enable reaching required concentrate quality with adequate recovery.

Geometallurgical models referred earlier generally almost solely ignore liberation information and the use of textural information is quite undeveloped.

In mineral processing the relationship between the mineral (micro) textures and liberation has been a separate research subject for a long time. Basically the aim has been to forecast the liberation distribution from a two-dimensional picture of an ore. This is generally called *the liberation model*. The principle was presented already in early 1900 by Gaudin (1939). Andrews and Mika (1975) developed a graphical presentation and this was further developed by King (1975) and King and Schneider (1998). These models assume random breakage which is unfortunately very rare especially in grinding. King and Schneider (1998) developed the model further and included a kernel function which overcomes the problem of random breakage. Gay (2004) used slightly different approach. Hunt et al. (2011a and 2011b) used chess-board pattern for crushed samples and reduced the effect of the random breakage assumption. All these methods require two dimensional microphotograph of an ore sample. In a geometallurgical context this means a preparation of thin sections, their photographing and image processing for a large number of samples. This is not very practical and an alternative way is needed.

This case study aims to find a solution how to incorporate mineral texture information into a particle based approach (Fig. 1) modified from a concept by (Lamberg, 2011). This is done through a case study of Malmberget iron ore deposit, in Northern Sweden. It focuses on mineral parameters, such as modal mineralogy, mineral textures, mineral association, mineral grain sizes and their relation to the liberation characteristics.

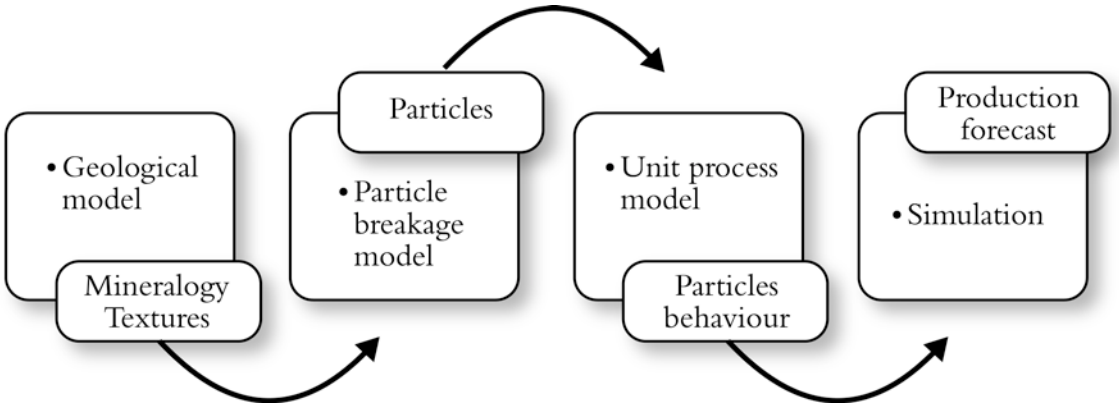

Fig 1. The particle-based geometallurgical concept modified from Lamberg (2011). Modal mineralogy and texture links the geological model and process model. In the process model minerals are treated as particles. From the geological information the particle population is generated through the particle breakage model.

The final purpose is to deliver a geological model which can offer quantitative rather than descriptive data to be used in a process model. Firstly, the geological model is complemented with textural information. Secondly, it is demonstrated how such geological model can be linked with a process model capable to forecast the metallurgical response like grade and recovery for any given geological unit (sample, block, or domain).

2 Sampling, experiment and analytical work

The samples in this study were collected from five drill cores representing two ore bodies, Fabian (Fa) and Printzsköld (Pz) in the Malmberget deposit. Sampling, sample preparation and analytical methods used for the mineral analyses and the element to mineral conversion are in detailed described by Lund et al. (2013).

Three dominate ore types were identified during logging, namely i) Feldspar (albite and orthoclase) rich ore (Fsp) of Fa and Pz, ii) Apatite rich or of Fa and Pz and iii) Amphibole rich ore of Fa, generating a total of >100 kg in five different composite samples.

The composite samples were processed and analysed at the LKAB, Malmberget laboratories. They were first crushed to a particle size below 3 mm. This was followed by a dry magnetic separation tests with Sala Mörtsell magnetic separation using standard test procedure by LKAB producing two outputs: concentrate and tailings (Lund et al., 2010). The test products were weighed and sized into ten size fractions using sieves of 38, 75, 150, 300, 425, 600, 1190, 1680 and 3000 microns. The size fractions were analysed for their chemical composition by X-ray fluorescence and SATMAGAN magnetic balance (Lund et al., 2013). Polished resin mounts were prepared for five finest size fractions (excluding 0-38 microns fraction) and analysed with QEMSCAN E430 Pro at LKAB, Luleå. The QEMSCAN data was exported into Excel files and read into HSC Chemistry for data processing.

The mineral textures were comprehensively characterised by optical microscopy with an attempt to develop a quantitative systematic besides the modal mineralogy, i.e. GEM-types. For that purposes the grain size of magnetite and the associating minerals were quantified in each texture.

The purpose of the processing of the mineral liberation data was to quantitatively track how different kind of multiphase particles deriving from different textural type behave in processing. For that purpose a particle tracking technique by Lamberg and Vianna (2007) was used. The Particle Tracking was done with HSC Chemistry software developed by Outotec (Lamberg et al., 1997). The algorithms of the Particle Tracking were also used in textural classification of the progeny particles, as described below.

Particle tracking uses mass balanced mineral by size data. Instead of using mineral grades by QEMSCAN, the modal analysis was done with element to mineral conversion technique and calculation procedure developed by Lund et al. (2013). Using HSC the raw mineral grades with solids flow rates data was first balanced on unsized basis (1D) and then for size by mineral basis (2D) with additional constraint that the 1D mass balance is conserved.

The QEMSCAN analysis gave a total of 16 minerals but to make this match with the mineralogy of element to mineral conversion some of the trace minerals were combined to more abundant phases (Lund et al., 2013). This gave a total of five most important minerals to be used in textural classification and in the particle tracking. After

combining the minerals, the next step of the Particle Tracking is to adjust the mass proportions of the particles to meet the mass balanced 2D modal composition. This stage adjusts the mass proportion of measured particles but does not change their composition. The adjustment for the liberation data is very small but is needed to make the particle data fully consistent with the 2D chemical mass balance. This means that if the modal and chemical composition of the size fractions and streams is back calculated from the adjusted particles the result is exactly the same as received from the 2D mass balance.

To mass balance particles they must be grouped somehow and in the particle tracking this is done by their composition. The basic binning stage groups particles for different binary and ternary combinations. In the system of five minerals plus others, i.e. six phases**,** and five size fractions after this step, the total number of particles in each stream was 2166. Some of the particle groups may have very few particles if any. Therefore, the advanced binning is a stage which combines established groups to ensure that each group has enough particles for sound mass balancing of particle groups. The liberation measurement is challenging in very fine (<10 micron) particle sizes, and in coarse size ranges the number of measured particles will be very small. Therefore, the Particle Tracking includes a step to extrapolate the liberation information (i.e. particles) for size fractions which have not been measured. In this study liberation was measured in five size fractions, and the remaining two size fractions were extrapolated.

After the previously described stages each process stream will be composed of similar particles classes but they are not in balance. The last step reconciles and mass balances the whole circuit for the given particle classes. This is done by keeping the total solids flow rate of the stream fixed and by minimizing the weighed sum of squares between measured and reconciled mass proportion of the particle classes. The particle tracking has an option for smoothing the data, but this step was not used in this study. The error analysis was done with Monte Carlo simulation which means that based on given standard deviations HSC drew a new dataset and solved the particle mass balance. This was done 100 times, and finally the standard deviation for the particle grades and recoveries was calculated.

3 Description of the textures

Textures are critical mineralogical characters in governing the ore behaviour in mineral processes. This is commonly accepted and has been widely known since decades (Butcher, 2010). But unanswered question is remaining how to describe textures and how to use the textural information in utilising the ore deposit and managing the production, e.g. in geometallurgy (Bonnici, 2008).

The geological definition for *textures* is: The relative size, shape, and spatial interrelationship between grains and internal features of grains in a rock (Spry, 1969; Fettes and Desmons, 2007). Textures, refers thus to a generally description on the small scale properties which mostly is in qualitative terms, e.g. pegmatitic texture, fined grained granoblastic texture. Descriptive mineralogical information, such this is insufficient in geometallurgy as it only gives possibilities to use the texture information for classification of different ore types. In geometallurgy this may lead to a great number of domains and for each of them separate sample sets need to be collected for geometallurgical/metallurgical testing. If, on the other hand, texture could be described numerically, and even

with additive parameters, this information could be processed with geostatistical methods and be used in a similar ways as the metal grades are currently used in resource estimation (Glacken and Snowden, 2001).

3.1 The Malmberget iron ore

The Malmberget iron ore deposit consists of several ore bodies of massive magnetite and hematite (Geijer, 1930) which are exposed for an extensive regional metamorphism and deformation, intruded by several generations of felsic and mafic dykes (Martinsson and Virkkunen, 2004). The magnetite and hematite ores are fully metamorphically overprinted seen as recrystallized coarse grained ore minerals, metamorphic textures, different oxidation textures and a chemical redistribution of elements between the magnetite and hematite. Compared to the well-known Kiirunavaara ore body, the Malmberget deposit is lower in tonnages, slightly lower in Fe grade and has a moderate but varying P content (Bergman et al., 2001). Mineralogically the iron ores are rather simple. Magnetite and hematite are the main ore minerals, and typical gangue minerals are apatite and amphibole-pyroxene.

In the massive ore a broad variation of mineral-textures can be identified. The magnetite has textural variations mainly in the magnetite grain size, grain shape and association. The texture is mostly granoblastic with distinct triple junctions at the grain boundaries. Coarse grained magnetite occurs as porphyroblasts or as veins in a finer grained matrix of magnetite. Larger magnetite grains can have an elongated shape following the mineral lineation in the host rock. In the western part of the deposit, hematite is the main mineral together with magnetite. Typical metamorphic textures are exsolutions patches of spinel in magnetite or oxidation surfaces of hematite. The magnetite grains show also intergrowth of ilmenite as lamellas or rutile needles.

In contrast to the massive ore semi-massive ore surrounds the ore bodies, particularly seen in the eastern part of the Malmberget deposit. The semi-massive ore has traditionally been called ore breccia (Geijer 1930). It is lower in Fe and higher in SiO_2 and can extend several tens of meters with a decreasing iron grade. The main non-iron minerals are the silicates i.e amphibole, feldspar (albite and orthoclase), quartz and biotite in various proportions that generate several different mineral assemblages with complicated textures.

The distinct chemical discrepancies of the massive ore and the semi massive ore are important to consider as the ore resource estimation uses traditional 3D block models which solely are based on the chemical analyses of the ore samples. The mass proportion amounts of semi-massive ore that is present in the process is consequently very significant and will not only influence the ore reserve estimation but also contribute to elemental variations in the mineral process. Therefore, a classification between the massive ore and the semi-massive ore can clarify the true distribution of the chemical elements from the valuable and the gangue minerals and give more precise information for defining the ore boundaries.

3.2 Textural classification

Using drill core logging (i.e. macroscopical observations) and optical microscopy an attempt was done to develop a classification based on the mineralogical and textural relation of the massive and the semi-massive ore. Textures were described and classified according to magnetite grain size and shape, generic mineral grain size and the main

associating mineral with magnetite (Table 1). The following textural types, arranged in the order of increasing magnetite grade, were identified: disseminated, veiny, patchy, banded, granules, speckled and massive.

Table 1. A classification scheme outlined for the massive and semi-massive ore from the Malmberget deposit based on the mineralogical and textural relation.

Ore type	**GEM-type**	**Fe-mineral**	**Fe grade ***	**Texture type**	**Sub type**	**Grain shape**	**Grain size, mean (µm)**	**Texture description**	**Main associating mineral to magnetite**
Semi massive ore	Fsp	Mag	<10 % (L)	Disseminated	Fine	Euhedral to anhedral	44	Fine grain magnetite occurs as disseminated in the silicate matrix	Fsp-Qtz
	Fsp, Bt-(Amph-Ap), Qtz bearing Fsp+Amph	Mag	10-80 % (L-H)	Veiny, patchy, banded, granules	Fine	Euhedral to anhedral	59-74	Mag grains, irregular distribution in the grain boundaries of the fine grain silica matrix or as smaller inclusions in fsp grain	Fsp-Qtz-Bt-Amph
					Coarse	Euhedral to anhedral	90-129	Mag grain occurs as single grains in grain boundaries or as aggregate often outlined in veins or patches in the matrix	
	Qtz bearing Fsp+Amph	Mag	>80 % (H)	Speckled	Coarse	Sub- to anhedral	133	Larger magnetite grain giving a semi-massive appearance	Fsp-Qtz±Amph
Massive ore	Amph-(Ap-Bt)	Mag	90-100 % (L-H)	Massive	Fine	Sub- to anhedral	100-200	Mag grain in a massive appearance as a compact equigranular matrix with coarser grains occurring as veinlike structure	Amph
						Euhedral	200-400		
	Amph-(Ap-Bt), Ap-(Amph)	Mag	90-100 % (L-H)		Medium	Subhedral	400-600	Mag grain occurs as granoblastic texture with distinct triple junctions at grain boundaries or as porphyroblasts (outline in linear direction)	Bt+Amph+Ap
						Euhedral	600-2400		
						Porphyroblasts	2000-3200		
	Ap-(Amph)	Mag	90-100 % (L-H)		Coarse	Euhedral	800-1400	Mag grain occurs as granoblastic texture with distinct triple junctions at grain boundaries. Elongated grains outline in a linear direction or as porphyroblasts give a brittle appearance	Ap

Clear dependence between the magnetite grain size and magnetite (i.e. Fe) grade was found (Table 1). In the low grade and disseminated texture ore the magnetite grain size is an average about 40 microns, and it increases through a semi-massive ore to 140 microns up to 1400 microns in the massive ore (Fig. 2, Table 1). Even this can be regarded as a general rule the massive ore and some textural types of the semi-massive ore show also variation in the magnetite grain size and can be further classified as fine, medium and coarse grained.

The feldspar (Fsp) GEM-type in the semi-massive ore shows the biggest variation in textural features. It basically consists of two different materials identified by their colour. Melanocratic magnetite rich material brecciates the leucocratic feldspar -rich magnetite-poor matrix. The melanocratic parts consist of magnetite, apatite and amphibole veins, bands or patches that may develop into networks in the leucocratic rock. The mineralogy of the

leucocratic brecciating rocks consists of a varying proportion of albite, orthoclase, quartz and biotite with minor magnetite (Table 2).

The magnetite grains in the leucocratic parts are smaller in individual samples in all textural variants than in the melanocratic parts as shown in Fig. 2. The difference is about 40-60 microns larger. In both leucocratic and melanocratic parts the magnetite grain size increases with magnetite grade, and in addition the overall magnetite grain size increases from type 1 to 7 (Fig. 2). The texture type 2 (banded) is deviating from the linear correlation and thus shows an uncertainty when the Fe-grade is low.

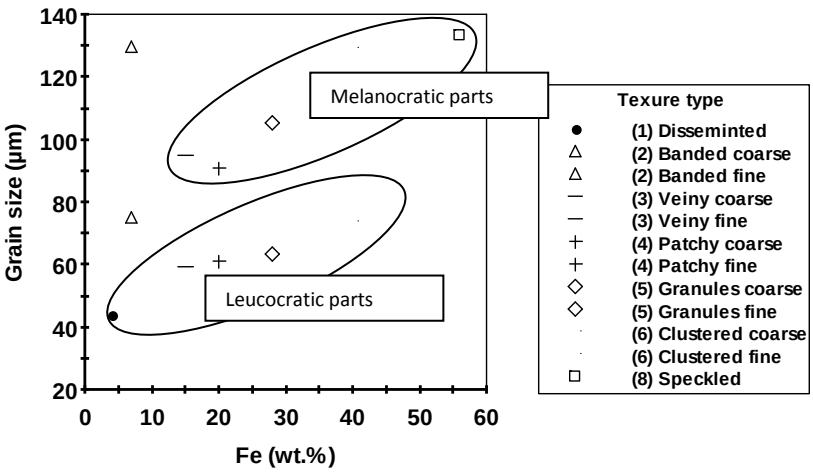

Fig. 2 Magnetite grain size – magnetite grade (Fe) shows a positive correlation in the Fsp GEM-type of Fabian ore. Fine grained and coarse grained form a bimodal system with two end members. The absence of texture type 7 is identified for Printzsköld ore body.

Table 2. Eight representative and different identified macrotextures of the classified Fsp GEM-type for different ore bodies in Fabian and Printzsköld ore bodies.

Texture type	***Sub-type***	***Picture*** *(Macro scale) (4 cm)* ↔	***Fine grain texture (Mgt-Fsp)*** ↔ *(Micro scale) (500 µm)*	***Coarse grain texture (Mgt-Fsp)*** ↔ *(Micro scale) (500 µm)*
(#) An increasing Fe-grade in the geochemistry analysis				
Disseminated (1)			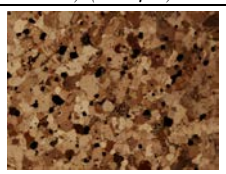	*Non existing texture*
Banded (2)			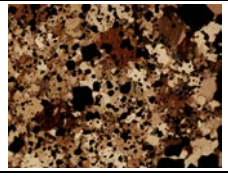	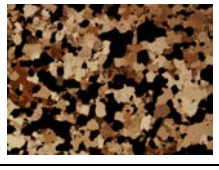
Veiny	*a)Waving veins (3)*		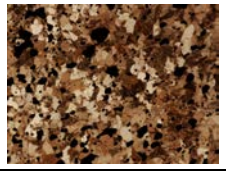	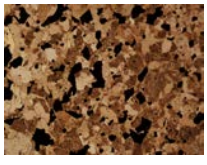

	b)Small veins (7) typical in Pz ore		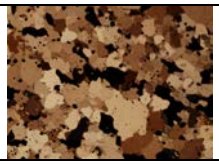	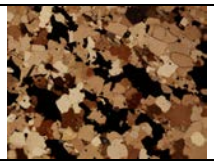
Patchy(4)			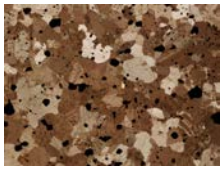	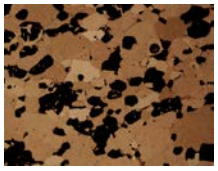
Granules (5)			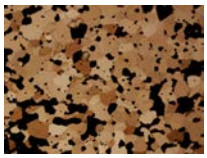	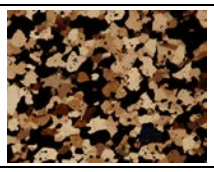
Clustered (6)			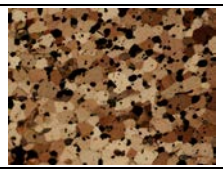	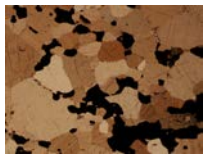
Speckled(8)			*Non existing texture*	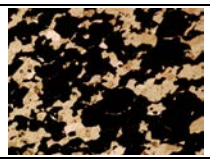

The Bt-(Amph-Ap) GEM-type is structurally controlled and is located in the footwall of the massive ore. Texturally, the Bt-(Amph-Ap) GEM-type is unique showing a schistose appearance due to the orientation of biotite. Tabular biotite grains, mainly (10-400 μm), sometimes as large as 2000 μm, occur disseminated or as a cluster that follows the lineation in the host rock either interstitially to a magnetite- or a silicate granoblastic matrix (Table 3).

The Py bearing Amph-(Ap-Bt) GEM-type contains a significant amount of sulphides. Single euhedral grains of pyrite and chalcopyrite are in general 5-200 μm in size, occasionally up to 4800 μm and occur as dissemination and in veinlets, at the grain boundaries or interstitially to magnetite. This texture occurs both in the massive ore but more commonly in the semi-massive ore. The composition of this GEM-type regarding the mineral texture and the modal mineralogy is closest to the the Amph-(Ap-Bt) GEM-type.

Two different GEM-types exist in the massive ore: Amph-(Ap-Bt) and Ap-(Amph). The Amph-(Ap-Bt) type shows wide variation in the amphibole (-pyroxene) grain sizes and grain shapes, and two end members can be identified. The coarser grained variant consists of large recrystallised amphibole (-pyroxene) grains occurring as a cluster (0.8-3.2 mm) enclosing smaller magnetite grains (Table 3). In the finer grain variant, amphibole grains (0.2-1 mm) occur interstitially to magnetite grains, either with or without the inclusion of small magnetite grains. In both types the magnetite grains are similar in size; the biggest difference between them is that in the coarse grained variant the magnetite grains also occur as inclusions in amphibole, whereas in the finer grained variant, the magnetite occurs in the grain boundaries. These two textures can easily be identified during the drill core logging due to the significant difference in amphibole grain size (Table 3). The Ap-(Amph) type is texturally

homogeneous and have an equally sized apatite and magnetite which are closely associated existing in a granoblastic or porphyroblastic texture (Table 3).

Table 3. Different ore textures that are identified and defined in massive and semi-massive ore.

Fine grain clustered (9)	
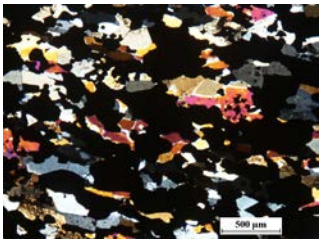 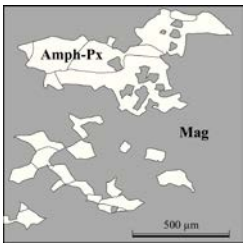	• Subhedral to anhedral magnetite grains (56-260 µm) occur in a granoblastic matrix with amphibole-pyroxene • Anhedral fine grain amphibole (25-180 µm) occurs interstitially to magnetite grains, either with or without the inclusion of magnetite grains (22-70 µm) • The grain size of the matrix is medium to coarse
Coarse grain clustered (10)	
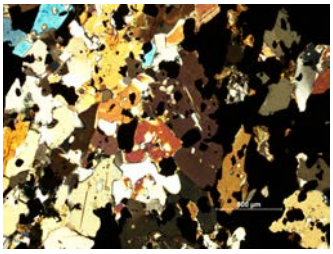 	• Single subhedral to anhedral magnetite grains (10-200 µm) occur interstitially in grain boundaries and as several inclusions in coarse or fine grained amphibole-pyroxene • The coarse amphibole grains exist as a cluster (800-3200 µm) or as fine single grains (80-100 µm) interstitially to magnetite • The grain size of the matrix is medium to coarse
Schistose (11)	
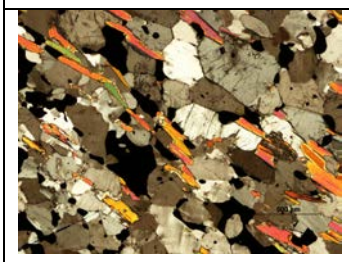 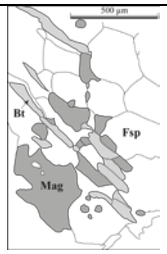	• Tabular single biotite grains (10-400 µm) occur as larger grains (up to 2000 µm), even a cluster or aligned in lineation interstitially to magnetite • The matrix is either a granoblastic magnetite or a silicate matrix • The grain size of the matrix is medium to coarse
Granoblastic texture (12)	
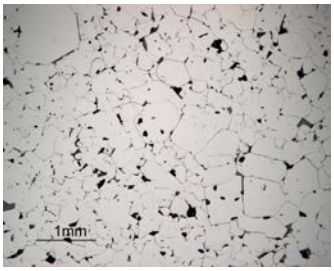 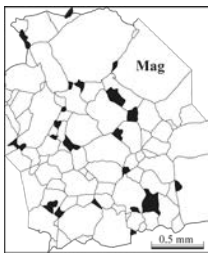	• Anhedral to subhedral magnetite grains occur either as a fine grained matrix (100-400 µm) or as a medium grained (400-800 µm) matrix • The magnetite matrix forms a dense texture sometimes giving a complex appearance of complicated grain boundaries • Other mineral associations are identified to have a porphyroblastic texture, such as magnetite-apatite, magnetite-ilmenite

Porphyroblastic texture (13)

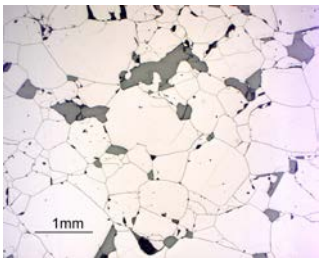

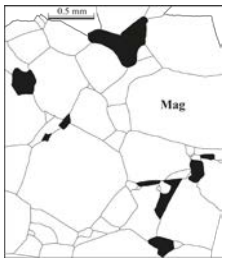

- Euhedral to subhedral magnetite grains (800-1400 μm) can have an elongated shape outlining a mineral lineation parallel to the general fabric of the rocks or occurring either as porphyroblasts (up to 4600 μm) or outlined in veinlike structures in the finer anhedral magnetite matrix
- The grain boundaries are simple and straight with clear triple junctions causing the rock to be brittle

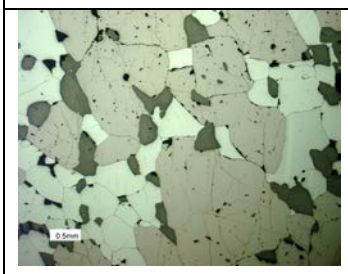

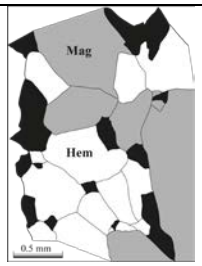

- Euhedral to anhedral (200-2000 μm) single hematite grains or as larger porphyroblasts (up to 20 mm) interstitial to magnetite grains
- Other mineral associations are identified as having a porphyroblastic texture such as magnetite-apatite, magnetite-ilmenite

Exsolution texture (14)

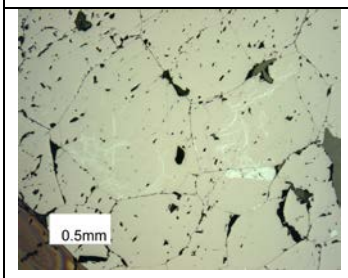

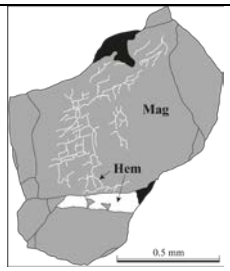

- Magnetite grains show oriented exsolved spinel patches (50-200 μm)
- Oxidation surfaces of hematite in magnetite grains or along the grain boundaries in the magnetite matrix

Lamella texture (15)

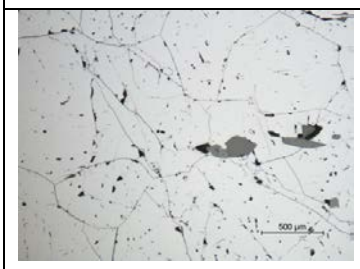

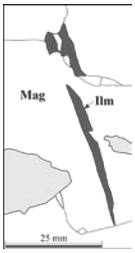

- Magnetite grains show intergrowth of ilmenite as oriented lamellas (trellis and sandwich) approx. (2 μm)
- Homogenous hematite grains have inclusions of (20-100 μm) Fe-Ti lamellas or as (10-50 μm) rutile needles at the rim of the grain

The combinations of the different mineral textures are unique for almost each GEM-type, but what is common that each of them has both a fine and a coarse grained variant (Table 4).

Table 4. The iron ore is classified into several classes and subtypes until unique categories of the mineral information is distinguished to be used in a geological model. The Fsp GEM-type is used for detailed mineral texture analysis.

Classified iron ore	**Ore type**	**Sub-ore type**	**GEM-type**	**Textures**
(2) Fabian	Semi-massive ore	Feldspar rich	Fsp	1-8, 11
	Massive ore	Amphibole rich	Amph-(Ap-Bt)	9-10, 12-15

		Apatite rich	Ap-(Amph)	12-15
(3) Printzsköld	Semi-massive ore	Feldspar rich	Fsp	1-8, 11
		Biotite rich*	Bt-(Amph-Ap)	11-13
	Massive ore	Apatite rich	Ap-(Amph)	12-15

*This sub-ore type not sampled

The textural study shows that when the mineral textures are considered the modal GEM-types divide into numerous types, and the closer one looks the more complicated and numerous the classes become (Table 4). In a geometallurgical context the use of classes is problematic since the treating of non-numeric data in block modelling is challenging. Therefore, to change the geological model from descriptive to practical mineral textures must be changed from qualitative to quantitative. Therefore, the mineral textures are now considered from the mineral processing viewpoint.

In mineral processing, ore is comminuted to liberate the minerals and to make the particle size suitable for downstream processes. Comminution is an energy intensive stage, and therefore a good balance is aimed between mineral liberation and throughput (i.e. used energy/feed tons). Full liberation is not a feasible target since besides high energy required the separation efficiency of downstream processes tends to decrease toward very fine particle sizes (<20 microns). Therefore, after the comminution stage the targeted degree of liberation for the ore minerals is typically 90-95% and different kinds of composite particles are present. A term liberation distribution is used here to summarise the information on mineral deportment; thus, it describes the distribution of particles by their composition (cf. particle size distribution).

In comminution, the ore is broken into particles using multiple stages of size reduction, such as blasting, crushing and grinding, and classification, like screening and hydrocycloning. The behaviour of an ore in the comminution is dependent on machine parameters, such as nature and magnitude of the applied comminution energy (unit operation properties and operational parameters), and on the material's physical properties, such as elasticity, hardness and strength. These together will define in a given process the relationship between specific energy (energy/mass) and overall size distribution of the material. The term grindability describes this, and it is the *measure of the specific energy consumption required to reduce a certain mass of material from a given fresh and initial size down to a defined product size by grinding*. Similarly, the term crushability is used for crushing.

Comminution circuits are designed and operated to provide targeted product fineness, and almost without exception this figure is fixed or changed very seldom. However, it is common that the grain size and association of the ore minerals vary within the ore body and therefore in plant feed on a daily basis. A good geometallurgical model should therefore not only forecast the metallurgical response but also give the best operational parameters, i.e. the target liberation degree and accordingly the target grinding fineness for any given rock unit or plant feed (blend).

The liberation distribution of a comminuted ore is dependent not only on (1) nature and magnitude of applied comminution specific energy and (2) crushability and grindability, but also on (3) modal mineralogy and (4) mineral textures. The first factor is independent of material. The three other factors cannot be separated fully from each other since the physical properties controlling the comminution behaviour are highly dependent on modal mineralogy and mineral texture. Since there are established techniques to experimentally determine the crushability and grindability and to use them in process simulations, the third factor is taken as an isolated parameter, and it gives together with the first parameter the overall particle size distribution of the material after comminution.

How does one decouple the effect of the modal mineralogy and texture into the liberation distribution? Firstly, the mineral grain size is basically a pure textural property, but as shown above the magnetite grain size has a positive correlation with the magnetite grade (Fig. 2). The associating mineral is controlled both by the modal mineralogy and the texture. In the Fsp GEM-type the association of magnetite in the melanocratic and leucocratic parts is different (Table 2). These examples show that the modal mineralogy and the mineral textures are intimately mingled with each other, and their separation using a traditional textural definition is practically impossible. Therefore, a new definition for mineral textures is given:

"Two samples are texturally different if the liberation distribution by size (compensated against modal mineralogy) is different after comminuted in similar conditions."

This separates the comminution properties and the modal mineralogy from the textural properties as well as states that for the textural classification, the liberation distribution must be compensated against modal mineralogy and studied by size.

3.3 Textural archetypes

By using the liberation distribution of the different GEM-types an attempt to quantify the mineral textures was done using samples including different textural types (Table 4).

All of these samples show a variation in the modal mineralogy by size fraction as illustrated by the magnetite grade by size in Fig. 3. This shows that the breakage is selective, and an attempt to forecast the liberation distribution from uncrushed samples by applying the random breakage model will fail. Also, the grade distribution varies by ore type. The Fsp GEM-types show an increase in the magnetite content by particle size. A similar pattern is found in the Ap GEM-types with an exception that the finest size fraction has the highest magnetite grade. Differing from the previous the Amph GEM-type shows the highest magnetite content in the middle size fractions, i.e. 75-150 and 150-300 microns. The variation in the mineral grade by size gives the first challenge when comparing the liberation distribution (Fig 3).

The degree of liberation of magnetite decreases in all samples by particle size (Fig. 3), which is logical and found almost always in ore samples. However, the overall liberation degree (of magnetite) can be different in the bulk sample even if the liberation degree by size is similar, if the overall particle size distribution if different. Therefore, the degree of liberation from the textural point of view must be studied by size. The Fsp GEM-types from Fabian

and Printzsköld show that clearly (Fig. 3): they have identical liberation degrees for magnetite in four size fractions, but in the size fraction 425-600 microns, the Fabian sample shows much better liberation. This causes the overall liberation degree to be different (Fig. 3).

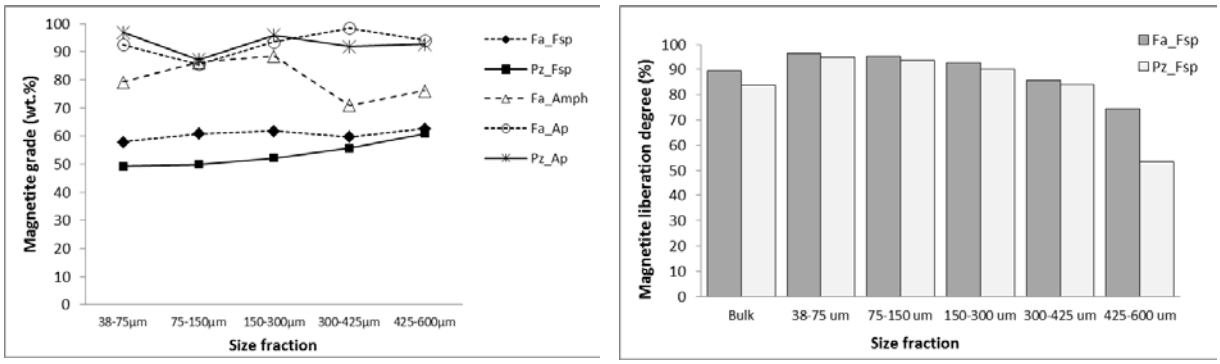

Fig. 3 The magnetite grade plotted against the particle size in five different GEM samples from Fabian (Fa) and Printzsköld (Pz) (left). The degree of liberation for magnetite by size fraction in the Fa_Fsp and Pz_Fsp samples.

In order to compare the liberation distribution of five different samples, a characteristic size fraction, 150-300 microns, was selected. The magnetite grade in the 150-300 microns size fraction is close to the bulk sample; the mass proportion in crushed sample was high enough and the number of particles measured gives sound statistics. In the size fraction the degree of liberation of magnetite has a positive correlation with the magnetite grade, but the Fsp-type differs significantly from the Amph- and Ap-types. In the Fsp-type the magnetite liberation is better than the grade would suggest (Fig. 4A).

The comparison of mineral association for non-liberated particles is challenging. If just comparing the mass proportion of magnetite with for example albite, the figure is affected by the magnetite liberation and the albite grade. If the liberation degree is high, the association of magnetite with albite must be low, and similarly if the albite grade is low the mass proportion of the binary magnetite-albite grains will also be low. Therefore, a new "Association Index" (AI) was developed. It aims to describe how common it is to find the target mineral locked with the other minerals regardless of the liberation degree and the modal composition. The association index is calculated for each mineral pair using the following formula:

$$AI_{A-B} = \frac{Mineral\ A\ deportment\ with\ mineral\ B\ (when\ fully\ liberated\ grains\ are\ excluded)\ [wt\%]}{Mineral\ B\ grade\ (in\ a\ phase\ excluding\ mineral\ A)\ [wt\%]}$$

If the association index of a mineral pair A-B is 1, then the association of mineral A with B is as common as the modal composition would suggest. If the association index is greater than 1, then the association is more common than expected, and if it is lower than 1 then it is rarer than expected. Index value zero shows that there is no association between minerals A and B.

Examples of the calculations of the associate index are given in Table 5. The three first factious samples show a similar association index with different modal compositions. Sample 4 shows that even if the deportment percentages are equally high for the pair A-B and A-C, the association index shows that A can be found relatively more often with phase C than with B. Sample 5 shows that the association index cannot be calculated for binary systems (C=0).

Table 5. Calculation examples for the association index. For the calculation modal [(1)-(3)] and deportment [(4)-(7)], the analysis result is needed.

Sample	1	2	3	4	5	(Row)	Formula
Modal composition (wt. %)							
A	50	40	50	50	50	(1)	
B	25	30	40	40	50	(2)	
C	25	30	10	10	0	(3)	
Deportment of the target mineral A, mass proportion (wt. %) of A in different particle classes							
Liberated A	90	80	90	90	90	(4)	
In binary A-B	3	10	8	3	10	(5)	
In binary A-C	3	10	2	3	0	(6)	
In ternary A-B-C	2	0	0	2	0	(7)	
Mass proportion of minerals in a fraction (phase) excluding the target mineral A (wt. %)							
B	50	50	80	80	100	(8)	100*(2)/[(2)+(3)]
C	50	50	20	20	0	(9)	100*(3)/[(2)+(3)]
Deportment of A excluding the liberated class (wt. %)							
with B	50	50	80	50	100	(10)	100*[(5)+(7)]/[100-(4)]
with C	50	50	20	50	0	(11)	100*[(6)+(7)]/[100-(4)]
Association index for A							
with B	1.000	1.000	1.000	0.625	1.000	(12)	(10)/(8)
with C	1.000	1.000	1.000	2.500	-	(13)	(11)/(9)

The association indexes of magnetite with feldspars (albite+orthoclase), biotite, amphibole and apatite are shown for the selected size fractions of five different textural types from the Malmberget iron ore in Fig. 4b. The Fsp GEM-types of Fa and Pz show quite similar association indexes. The association index of magnetite with feldspar ($AI_{Mgt-Fsp}$) is smaller than 1, which means that magnetite is locked with feldspar less often than the modal mineralogy would suggest. On the other hand the association index of magnetite with amphibole ($AI_{Mgt-Amph}$) is higher than 1 showing that the magnetite is met more often locked with amphibole than the modal mineralogy would suggest. The association index of magnetite with apatite shows a significant difference between the Fsp and Amph (and Ap) GEM-types. In the Fsp GEM-types the magnetite is rarely occurring with apatite, but in the Amph and Ap GEM-types association is more common than the modal composition would suggest.

Because the association index is calculated for particulate material, it carries information on both the mineral textures (grain size, shape, associating mineral) and the ore breakage. This is clearly illustrated in Fig. 4c which shows the variation of the association index by size. If the texture is fully homogenous and the breakage fully

random, the association indexes should be 1 for all minerals in all sizes. Deviation from 1 can be due to heterogeneous textural or non-random breakage. The association indexes approach 1 as the particle size gets coarser, as shown in Fig. 4d for the Fsp GEM-type. This is because in coarse particle sizes the particles start to be identical in their modal composition and liberation distribution. This point is not reached yet at the 425-600 microns particle size for Fsp GEM-type sample of Fabian because the liberation degree of magnetite is as high as 74% (Fig. 3).

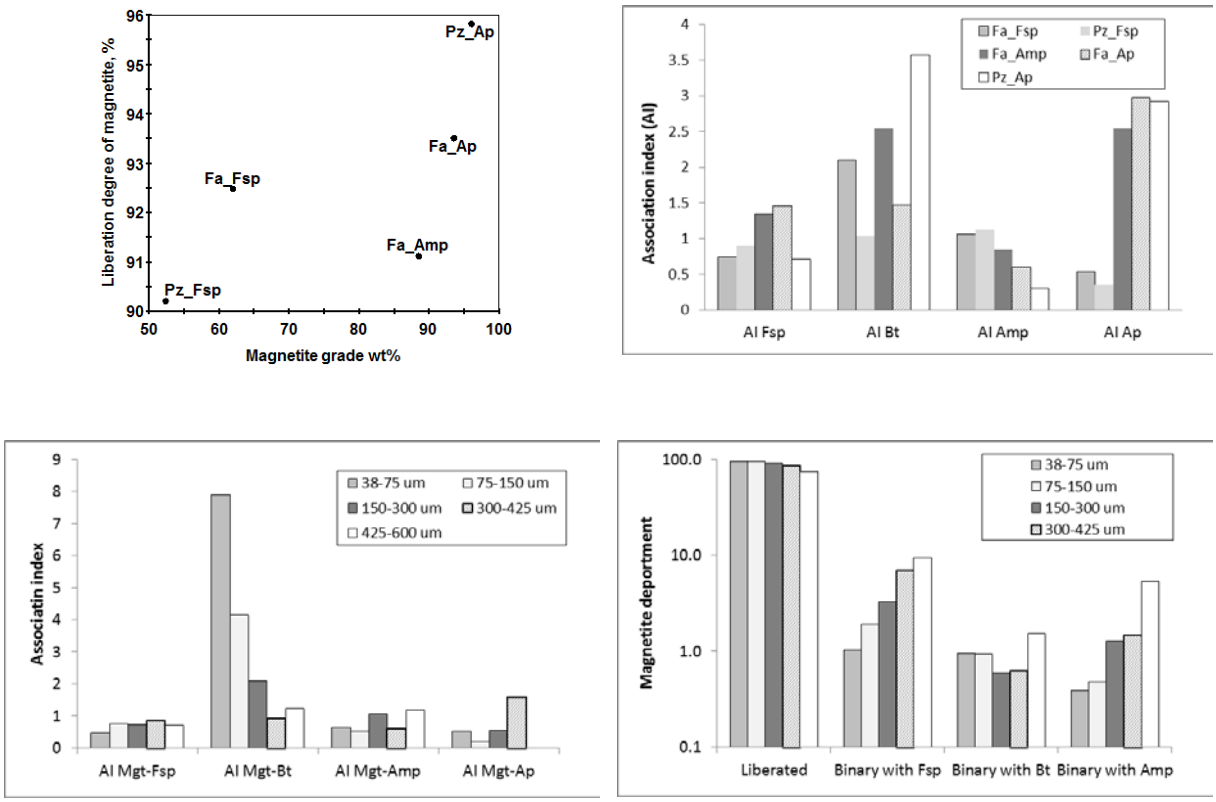

Fig. 4 **A)** The degree of liberation for magnetite versus the magnetite grade of three different GEM-type textures (Fsp, Amph and Ap) representing the size fraction, 150-300 microns (top left). **B)** The association index (AI) for magnetite in size fraction 150-300 microns in the same GEM-type texture (top right). **C)** The association index of magnetite in sample by size from Fa_Fsp fractions. **D)** The deportment of magnetite in sample by size fractions from the Fabian Fsp GEM-type.

The decoupling of the texture and breakage is not possible with the association index. Some more information is needed, and therefore the association index values are compared to the textural description of original uncrushed ore samples. The Fsp GEM-type consists of leucocratic and melanocratic parts and the magnetite and amphibole content is higher in the latter and feldspar grade is higher in the former. Association index values for magnetite with feldspar ($AI_{Mgt-Fsp}$) lower than 1 and higher values with amphibole ($AI_{Mgt-Amph}$) can therefore be explained based on the texture. Additionally, the variation in the association index of magnetite with apatite between the GEM-types can be explained from textural differences. In the Amph GEM-type, apatite preferentially occurs in contact with magnetite, but this is not the case in the Fsp GEM-type.

The association index of magnetite with biotite shows strong variation by particle size: in fine particle sizes the value is very high and decreases by size. Since biotite does not show a preferential association with magnetite in the original uncrushed ore samples, this must be a breakage feature. Thus, it is significantly more common to find magnetite locked with biotite in fine particle sizes than in coarse sizes, and this is not because biotite is more common in fine size fractions. Therefore, it indicates rather that magnetite-biotite particles don't break preferentially through grain boundaries rather the opposite.

Coming to the definition of texture, the Fsp GEM-types of Fabian and Printzsköld can represent similar textures since the liberation degree of magnetite and association indexes do not differ from each other strongly. The Fabian Amph and Ap GEM-types are also potentially similar in texture, and the Printzsköld Ap GEM-type is a textural type of its own. The question remains how small or big the difference between the liberation distributions and the related key figures used here (degree of liberation and association index) should be to justify saying that two samples are similar or different in their textures? In addition how this information will be gathered and used in a geometallurgical context?

To extend the modal compensation also into liberation degree, the calculation algorithms of the particle tracking technique were applied (Lamberg and Vianna, 2007). The particle tracking technique is for mass balancing the liberation data, but for doing that it includes steps where the particles are classified in a systematic way (basic binning and advanced binning), and the modal composition of the liberation measurement is refined to match with the modal composition calculated by the element to mineral conversion. Therefore, the liberation data of five samples was classified (basic binning) producing an identical particle population in each sample. After this, the liberation distribution of each sample was forecasted using the textural information from another sample. For this an algorithm given in Table 6 was used (Lamberg and Lund, 2012). For example, to forecast the liberation distribution of sample A from sample B (called archetype), the liberation spectrum of the archetype (sample B) was taken, and it was refined by using the modal composition of sample A.

Table 6. Adjusting the modal composition in generating the particle population based on archetype for given ore sample or block (Lamberg and Lund, 2012).

The particle population for a given sample is calculated by taking the particle population of the corresponding archetype. This is now iteratively adjusted, and for the adjustment, a correction factor, k, is calculated for each mineral (i) in a size fraction before each iteration round:

$$k_{i,fraction} = \frac{M(i)_{fraction}}{\sum_{j=1}^{n}(p(j)_{fraction} \times x(i)_p)}$$

Basically the formula above is a ratio of mineral grade from the geological model (M(i)) and the mineral grade back calculated from the liberation data of the archetype (denominator). p refers to mass proportion of particle in a size class and x(i) is the mass proportion of mineral in a particle.

The mass proportion of particle j (p_j) is recalculated on each iteration round using the correction factor and an equation:

$$p_{j,fraction} = p_{j,fraction} \times \sum_{j=1}^{L}(x(i)_j \times k_{i,fraction})$$

Using equations given above, the particle mass proportion is iteratively adjusted until the difference between mineral grades of the geological model and archetype has reached the required tolerance.

The results of the magnetite deportment of one pair Fa_Fsp and Pz_Fsp is given in Table 7. The algorithm forecasts the liberation distribution well in all other size fractions except in the coarsest 425-650 microns. This is most probably due to the small number of particles measured (about 400).

Table 7. The magnetite deportment measured and estimated using the Pz_Fsp and the difference between the estimated and measured.

		Bulk	38-75 um	75-150 um	150-300 um	300-425 um	425-600 um
Measured	Mgt Lib	89.4	96.4	95.2	92.5	85.6	74.3
	Mgt-Fsp	6.6	1.4	2.9	4.7	10.8	14.2
	Mgt-Bt	1.1	1.4	1.2	0.8	0.8	1.7
	Mgt-Amph	2.0	0.6	0.5	1.5	1.8	5.9
	Mgt-Ap	0.4	0.0	0.0	0.1	0.3	2.1
Estimated using Pz_Fsp	Mgt Lib	90.7	96.2	95.9	91.5	87.3	86.7
	Mgt-Fsp	7.0	2.1	2.4	5.7	10.8	10.6
	Mgt-Bt	0.9	0.6	1.0	1.7	0.1	0.5
	Mgt-Amph	0.8	0.8	0.4	0.6	1.1	1.2
	Mgt-Ap	0.1	0.1	0.2	0.1	0.0	0.0
Difference	Liberation	1.3	-0.2	0.8	-1.0	1.7	12.4
	Average	0.4	0.2	0.2	0.4	0.4	2.8

Fig. 5 shows the error in forecasting the liberation distribution with all of the combinations of the five samples. Putting a limit that the average error must be lower than 1%, and then the five samples can be simplified into two textural archetypes: Fsp and Amph/Ap. One sample from both groups is selected to represent the group, and this sample is called a textural archetype.

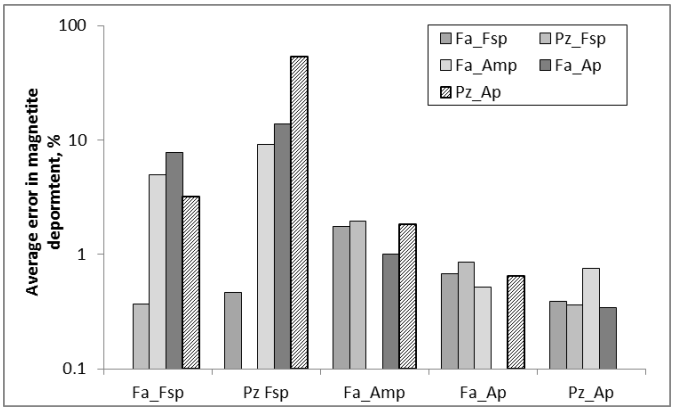

Fig. 5 The average error showing the magnetite deportment in the samples.

4 Framework for a metallurgical model

The process model takes the information of the geological model and transfers it to forecast on the metallurgical performance. When developing a metallurgical model, one needs to answer questions, such as: (1) what is the purpose of the model? (2) What is the level of the complexity of how material (ore) is described? (3) And how detailed is the information that the model can provide on a metallurgical performance?

In a geometallurgical context the purpose of the model is to return important metallurgical parameters in the resource (block) model. Typically in the processing plants this would include information like throughput, concentrate quality, recovery of the commodities and the tailing quality. In the case of Malmberget, the metallurgical parameters considered by the process model are (1): throughput, recovery of iron and concentrate grade in terms of iron, phosphorous and silica. The tailing quality is not a limiting factor in Malmberget, and there is no need to include that in the model.

In this study the geological model describes the resource on a mineralogical basis, and the process model logically uses the same approach. Three different levels can be used (2). The unsized, 1D, level uses minerals on an unsized basis, which means that there is no information on the particle sizes available. The sized, 2D, level uses the mineral by size for the material description and for the process models. This enables including particle size and the metallurgical functions can be size dependent. The liberation, 3D, level uses liberation information. Therefore, the process must describe the behaviour of particles by their composition and size.

(3) The level of processing details means how detailed the process is described in terms of unit operations and operational parameters. In the lowest level, one black box represents the whole process and no operational parameters are included. In the other end of the complexity lies a model where all unit operations are described and all effective operational parameters are included.

In this study the feasibility of the mineralogical approach is tested using a simple process: the one stage dry magnetic separation (cobbing) test for the Fsp GEM-type of Fa and Pz ore (Fa_Fsp and Pz_Fsp). The process model is developed for all three levels, namely 1D, 2D and 3D.

To reach the 2D level of the modal mineralogical, a mass balancing needs to be done on a size fraction level. The readers are referred to (Lund et al., 2013) for the calculation rules and detailed results. The 3D level was reach by the liberation analysis of the concentrate and tail and was then mass balanced using the Particle Tracking technique.

4.1 Comminution – particle breakage model

The particle brakeage model gives the liberation distribution of a sample when the information on corresponding textural archetype and modal composition is given (Fig. 6 and 7). The model converts 1D, i.e. unsized modal composition, to 3D (liberation distribution) using a textural archetype as a basis and a simple algorithm in adjusting the liberation data of the archetype to match with the given modal mineralogy. The textural archetype

also includes the information on how the modal composition varies by size. The overall size distribution model developed in a M.Sc. thesis by Koch (2013) was used.

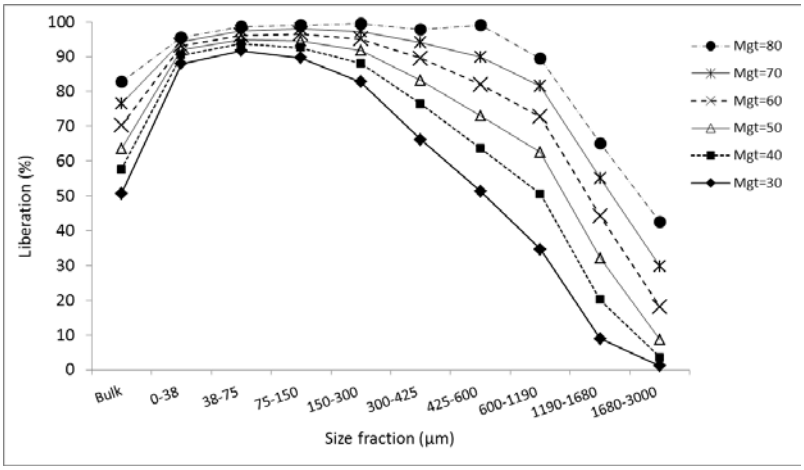

Fig. 6 The mass proportion of fully liberated magnetite in different size fractions as the magnetite grade in the ore varies between 30 and 80 wt%. The bulk refers to combined size fractions.

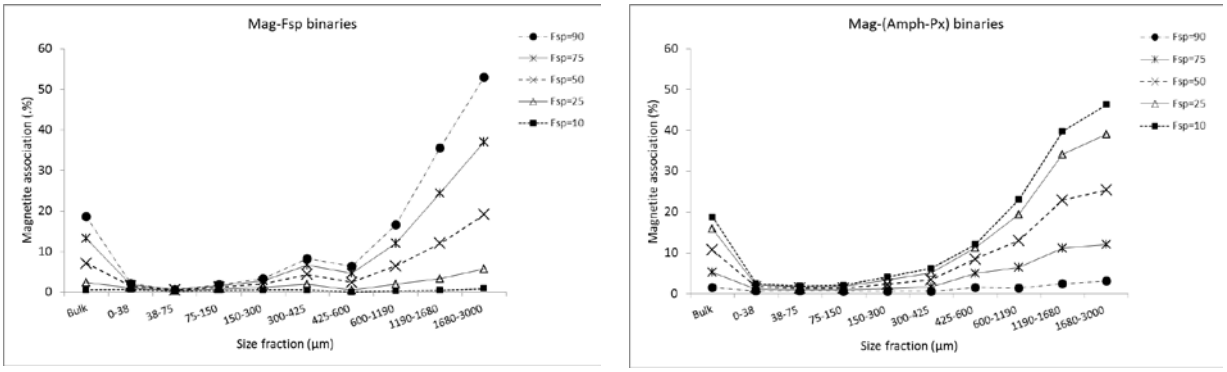

Fig. 7 The mass proportion of magnetite is shown in a magnetite-feldspar binary (left) and a magnetite-(amphibole+pyroxene) binary (right), as the ratio of feldspar to (feldspar+amphibole+pyroxene) varies between 10% and 90%. The bulk refers to combined size fractions. The magnetite grade is 50 wt%.

4.2 Concentration model – dry magnetic separation

The process model describes quantitatively the particle behaviour in each unit process stage and therefore returns the metallurgical response (grades for Fe, Si and P and recovery for Fe) for any given geological unit (sample, block, domain). In the minerals processing the behaviour of particles is dictated by the particle properties; therefore, the unit models have to include the particle properties, such as size, composition and density. The structure of the simulator binding up the unit models must be based on particles (Lamberg, 2011).

The unit operations models used in minerals processing can be divided into four types: 1) Comminution models where particle size distribution changes. 2) Separation models where particles are distributed between two or more output streams based on their physical properties. 3) Leaching and precipitation models where the liquid

phase is an active component and minerals dissolve and new phases are formed through chemical reactions. 4) Simple mixers and mass distributors where material is mixed and distributed between the outputs.

In the comminution unit models (grinding mills, crushers), it is possible to use the particle breakage model described above. Therefore, in the model the forecasting of the liberation distribution and the total size distribution can be decoupled. In the latter the traditional populations balance breakage models can be used (Weller et al., 1996: Alruiz et al., 2009; Vogel and Peukert, 2003).

Most of the separation and leaching models used in industry are semi-empirical. In minerals processing the fundamental process model based entirely on physics, chemistry and particle properties are still quite far away from being practical and accurate enough for everyday use. The development of property based models in minerals processing requires that particle properties can be measured in different parts of the process. For this the liberation analysis is a state-of-the-art technique (Sutherland and Gottlieb, 1991; Gu, 2003; Fandrich et al., 2007), and X-ray tomography is an emerging method (Miller et al., 2003).

The liberation measurement gives the quantitative information on the particles in a process stream, but for modelling purposes liberation data must be mass balanced. This is done by the Particle Tracking Technique (Lamberg and Vianna, 2007), a quantitative description of how different particle types (liberation classes) behave in single process units and in a full process.

For the Malmberget concentration process, the first unit model was developed for the dry magnetic separation stage, i.e. cobbing. Fig. 8 shows the distribution of minerals on an unsized basis between the concentrate and tailing for the Fsp GEM-type from Fabian. In a particle size of P80 = 1 mm, about 30% of the material is rejected into the tail (MagTail) with about 6% magnetite losses, i.e. the recovery of magnetite into the magnetic concentrate is 94% (Fig. 8).

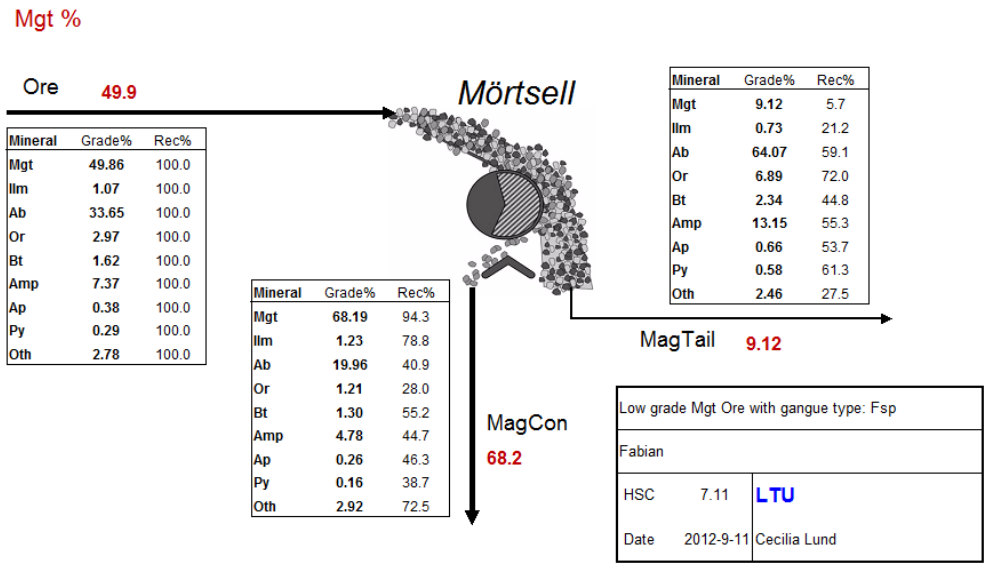

Fig. 8 The processed mineral grade and recoveries in a Mörtsell dry magnetic separation (cobbing) test from for the Fsp GEM-type of the Fabian ore type.

Studying the behaviour of the minerals by particle size it can be seen that for magnetite the recovery is quite constantly between 92 to 96% in particle size range from <38 microns to >1.68 mm (Fig. 9). All of the gangue minerals show a similar pattern having the recovery minimum between 38 and 106 microns (Fig. 9). Noteworthy is that the biotite shows higher recoveries than the other gangue minerals, especially in the finest particle size fraction <38 microns. Also, minerals show a significant difference in particle sizes coarser than 500 microns; albite shows clearly the lowest recovery, whereas apatite and biotite the highest. Excluding the finest size fraction, the mineral recoveries can be explained by their association with magnetite (Fig. 9). Therefore, the different patterns found for each mineral in their recovery by size are due to their liberation distribution and the association with magnetite.

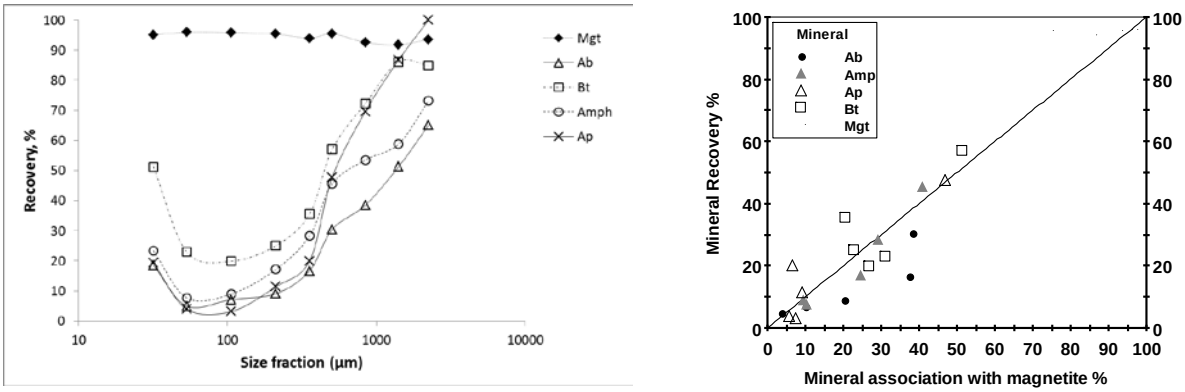

Fig. 9 The cobbing test with a sample from the Fsp GEM-type of Fabian shows the recovery of minerals by size (left). The mass proportion of minerals associated with magnetite vs. mineral recovery where five size fractions between 38 and 600 microns are shown. The fully liberated grains are shown for magnetite (right).

Entering into the liberation level, it is obvious that magnetite rich particles enter into the magnetic concentrate, whereas particles rich in gangue minerals are found in the tailing (Fig. 10). The particle tracking technique, however, gives quantitative information on the behaviour of the particles.

Table 8. QEMSCAN pictures of typical particles from the magnetic concentrate and tail, Fabian Fsp GEM-type samples. Brown is magnetite, orange is feldspar.

Ore type	**Size fraction (microns)**	**Concentrate**	**Tail**
Fsp GEM-type, Fabian ore body	425-600	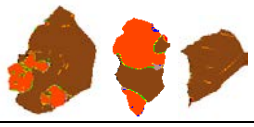	
	300-425		
	150-300		
	75-150		
	38-75		

Fig. 10 shows the recovery of magnetite-feldspar binaries into the magnetic concentrate by size and as a function of the magnetite grade. Interestingly, the recovery curve is upward convex in fine particle sizes and straightens toward the coarse particles.

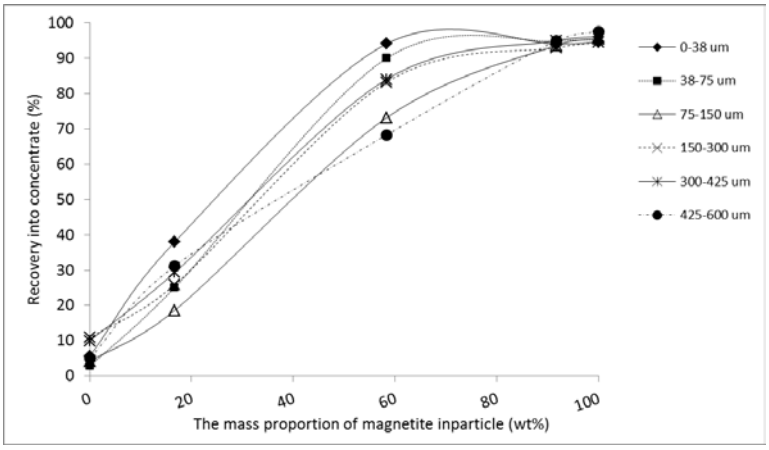

Fig. 10 The recovery of the magnetite-feldspar binary particles into the magnetic concentrate by size fraction as a function of magnetite grade in the particle.

The recovery curves are deviating only little from the linear; therefore, for simplicity a linear model was used. For the simulation of the magnetic separation the split values for each liberated minerals were given (Table 9). The basic assumption behind the model is that particles with a similar composition and size will behave in the process in a similar way regardless of from which part of the ore they are derived. The simulation was done using HSC Sim, and for multiphase particles the software uses the weighted average of the split values given for the liberated minerals.

Table 9. A model for the dry magnetic separation. Split values for minerals by size when occurring fully liberated.

Fraction	Magnetite	Feldspar	Biotite	Amphibole	Apatite	Others
38-75 um	0.961	0.030	0.109	0.035	0.031	0.331
75-150 um	0.965	0.033	0.048	0.064	0.012	0.651
150-300 um	0.971	0.054	0.088	0.090	0.104	0.554
300-425 um	0.971	0.042	0.000	0.148	0.000	0.410
425-600 um	0.987	0.112	0.000	0.371	0.047	0.856

Three cases were simulated (Table 10). In the first one Fa-Fa, the feed material was from Fabian, and the Fabian process model (split values in Table 9) was used. In the second one called Pz-Fa, the feed material is from the Printzsköld, and the Fabian model is used. In the third simulation, the Fabian sample was used as a textural archetype, and the Printzsköld modal composition was used to generate modelled Printzsköld feed. Also in this simulation the Fabian model was used (Pz(Fa)-Fa). The linear model (Fa-Fa) introduces a small error, the standard deviation of the difference for grade is only 0.29% and for recovery 1.3% (Fa-Fa). The Fa model succeeds to forecast the metallurgical performance for Pz when the liberation information is readily available: the standard deviation of the difference for grades is 0.93% and for recovery 2.7% (Pz-Fa). When the liberation information is not available and the feed sample is generated from the textural archetype, the forecast is still reasonably good; the

standard deviation of the difference in grades is 0.92% and the recovery 5.5%. These error levels clearly fulfil the need that the relative error should be below 5% for technical sampling and estimations. Therefore, the conclusion based on the limited testing is that the approach could be used for producing metallurgical parameters into the block model.

Table 10. The observed grades and recoveries in the magnetic concentrate in the cobbing test. The results are the sum of the size fractions from 38 to 600 size fractions. Diff: Difference (Sim-Meas), R.Diff: relative difference = 100*(Sim-Meas)/Meas.

Sample-Model Case	Fa-Fa				Pz-Pz				Pz from Fa archetype - Fa			
	Meas	Sim	Diff	R.Diff%	Meas	Sim	Diff	R.Diff%	Meas	Sim	Diff	R.Diff%
Mgt wt%	89.7	90.2	0.6	0.6	87.6	88.9	1.3	1.4	87.6	87.2	-0.4	-0.5
Fsp wt%	5.63	5.28	-0.35	-6.24	7.11	5.33	-1.78	-24.99	7.11	5.59	-1.52	-21.34
Bt wt%	0.85	0.76	-0.08	-9.57	1.24	1.71	0.47	38.14	1.24	2.95	1.71	138.21
Amp wt%	2.14	2.12	-0.02	-0.95	1.83	2.06	0.23	12.70	1.83	2.54	0.71	38.71
Ap wt%	0.09	0.10	0.01	5.60	0.58	0.85	0.28	47.73	0.58	0.79	0.21	36.33
Fe wt%	65.4	65.8	0.4	0.6	63.9	64.8	1.0	1.5	63.9	63.7	-0.2	-0.3
Si wt%	2.58	2.44	-0.14	-5.33	3.06	2.64	-0.43	-13.90	3.06	3.10	0.04	1.27
P %	0.01	0.02	0.00	7.66	0.09	0.14	0.04	48.08	0.09	0.13	0.03	36.69
Mgt Rec%	94.9	93.0	-1.8	-1.9	91.6	92.6	1.0	1.1	91.6	90.9	-0.8	-0.8
Fsp Rec%	13.0	11.9	-1.1	-8.6	17.0	12.7	-4.3	-25.2	17.0	13.3	-3.7	-21.6
Bt Rec%	30.5	26.9	-3.6	-11.8	8.6	11.9	3.2	37.7	8.6	20.5	11.9	137.5
Amp Rec%	20.0	19.3	-0.7	-3.5	16.9	19.0	2.1	12.4	16.9	23.4	6.5	38.3
Ap Rec%	13.4	13.8	0.4	3.2	4.9	7.2	2.3	47.2	4.9	6.6	1.8	35.9
Std grade			0.29				0.93				0.92	
Std Rec			1.3				2.7				5.5	

As the process model is based on the particle properties, the model can be used more widely than traditional unit models which need to be calibrated if there is a change in size distribution, modal mineralogy or liberation.

5 Discussion

This is the first geometallurgical model of the Malmberget iron ore deposit based on a mineralogical approach which is developed in three separate steps.

In contrast to the developed geometallurgical concept by Niiranen and Böhm (2012) which is based on geometallurgical and metallurgical testing using the Kiirunavaara deposit as a case study, the geometallurgical model developed here aims to be a complementary and partly an alternative way. As this study uses mineralogical approach and generic tools the methodology can be applied directly in other ore types and commodities. It demonstrates that when the geological model relies on a proper ore characterisation and provides high-level quantitative mineralogical data the information is adequate (without elemental grades) to be used in the resource estimation and in the block model.

The benefit of a described geometallurgical model is that it enables to optimise and forecast the production on a long term basis (Lamberg, 2011). To get the full benefit the model should be established already in a feasibility stage. For deposits in production, like Malmberget, the geometallurgical model can instead be used to recognise

the process limitations and re-evaluate the mining plan. It facilitates also the possibility to make realistic process predictions which potentially improve the performance by giving on daily basis useful and achievable production targets.

To use modal mineralogy in geometallurgical classification for some weathered iron ores has shown to be useful before (Paine et al., 2011; Neumann and Avelar, 2012) but the quantification and usage of mineral textures is still a challenge and so far quite undeveloped. There are some new methods to produce the mineralogical and textural data, rapidly and inexpensively (Hunt et al., 2009, 2011; Bonnici et al., 2008, 2009; Perez-Barnuevo et al., 2012) and even use the textural information in modelling (Hunt et al., 2012). These methods are based on optical image system which also addresses a more inexpensive alternative than the use of automated mineralogy systems. The benefit of using the developed textural archetypes to distinguish different mineral textures would be an even more cost-effective analysis as it aims to identify the textural variants during drill core logging. This was outside the scope of this study and must be developed pointing that there is urgent need to develop better characterisation tools and analytical techniques to semi-automatically handle large amount of samples and routinely identify different textures directly on drill cores (Pirard et al., 2008; da Costa et al., 2009; Haavisto and Kaartinen, 2009).

The developed approach using textural archetypes needs still further development. How to identify if two samples are texturally different and how different they must be to justify calling them different textural archetypes? More testing is needed whether the particle breakage model can reliably forecast the liberation distribution. Also it is still largely unknown how good the estimate on metallurgical performance must be in order to be useful.

Using the modal mineralogy, a geometallurgical ore type (GEM-type) classification system was developed which capture the most important features like the iron mineral grade, iron mineralogy and the gangue mineralogy. This was to overcome the problem that the accuracy of the modal mineralogy by element to mineral conversion was not as good as required (Lund et al., 2013). As the geometallurgical model uses mineral grades, the error in the modal mineralogy is currently too high to be used in resource estimation (Pitard, 1989) and this need to be further developed before to it can be applied as a process tool.

The developed metallurgical framework gave the opportunity to follow the particles and identify what types of texture that matters in the process. Even if this geometallurgical model is based on a limited mineral process (one separation step), an important questions to answer is if it still is possible to see some textural impact in the final concentrates? Parameters that is not included in the model and needs to be considered and further developed is, in addition to a concentration model, also a comminution model that handle the variation in hardness and throughput. More textural archetypes including more particle size fractions need to be tested.

6 Conclusion

In this paper a geometallurgical model using the Malmberget iron ore deposit as a case study was developed. The main focus was the development of a method to quantify mineral textures which is one of the basic requirements to define the geological model. Firstly, this was solved by a descriptive classification scheme for identification of the mineral textures which also was used to verify the accurateness of the developed textural archetypes. Secondly, to quantify the mineral textures, a method was developed to describe and distinguish quantitatively different

mineral textures. This was done by processing the liberation data and decoupling the mineral liberation and associations from the modal composition. In the recognition of unique textures two key figures were used, namely the degree of liberation and the association index (AI). Each unique texture is collected in a library and an individual member of it is called textural archetype.

Finally, the geometallurgical framework and the geological model were tested comparing the forecasted metallurgical key figures against the ones received by metallurgical test. The difference in terms of product quality (Fe, Si and P grade) and in iron recovery were reasonable small validating the developed methodology

7 Acknowledgements

This project is financial supported by the Hjalmar Lundbohm Research Centre (HLRC), which we are thankful for. The authors want to express their gratitude to people at the LKAB for their contribution of data and knowledge. Åke Sundvall, Magnus Stafstedt, LKAB are acknowledged for comments and support.

8 References

Alruiz, O.M., Morrell, S., Suazo, C.J. and Naranjo, A., 2009, A novel approach to the geometallurgical modelling of the Collahuasi grinding circuit: Minerals Engineering, v. 22, p. 1060-1067.

Andrews, J.R.G. and Mika, T.S., 1975, Comminution of a heterogeneous material: development of a model for liberation phenomena: In Proceedings of 11th International Mineral Processing Congress, Cagliari, Italy, 20-26 April, Proceedings, p. 59-88.

Bergman, S., Kübler, L. and Martinsson, O., 2001, Description of regional geological and geophysical maps of northern Norrbotten County (east of Caledonian orogen): SGU Geological Survey of Sweden, v. Ba 56, p. 110.

Bonnici, N., Hunt, J., Berry, R., Walters, S. and McMahon, C., 2009, Quantified mineralogy and texture: Informed sample selection for communition and metallurgical testing: The Tenth Biennial SGA Meeting, Townsville, Australia, 17th- 20th August, Proceedings, p. 679-681.

Bonnici, N., Hunt, J., Walters, S., Berry, R. and Collett, D., 2008, Relating Textural Attributes to Mineral Processing - Developing a More Effective Approach for the Cadia East Cu-Au Porphyry Deposit: Ninth International Congress for Applied Mineralogy, Brisbane, Australia, 8-10 September, Proceedings, p. 415-418.

Bulled, D. and McInnes, C., 2005, Flotation plant design and production planning through geometallurgical modeling Publication Series, pp. 809-814.: Australasian Institute of Mining and Metallurgy, v. Publication Series, p. 809-814.

Butcher, A., 2010, Chapter 4 - A practical Guide to Some Aspects of Mineralogy that Affect Flotation, Flotation Plant Optimisation, Spectrum Series 16, p. 83-93.

da Costa, G.M., Barrón, V., Mendonça Ferreira, C. and Torrent, J., 2009, The use of diffuse reflectance spectroscopy for the characterization of iron ores: Minerals Engineering, v. 22, p. 1245-1250.

David, D., 2007, The importance of geometallurgical analysis in plant study, design and operational phases., v. Australasian Institute of Mining and Metallurgy Publication Series, p. 241-247.

Dobby, G., Bennett, C., Bulled, D. and Kosick, X., 2004, Geometallurgial modeling – The new approach to plant design and production forecasting/planning, and Mine/Mill Optimization: Proceedings of 36th Annual Meeting of the Canadian Mineral Processors, Ottawa, Canada, 20-22 January, Proceedings, p. paper 15.

Fandrich, R., Gu, Y., Burrows, D. and Moeller, K., 2007, Modern SEM-based mineral liberation analysis: International Journal of Mineral Processing, v. 84, p. 310-320.

Fandrich, R.G., Bearman, R.A., Boland, J. and Lim, W., 1997, Mineral liberation by particle bed breakage: Minerals Engineering, v. 10, p. 175-187.

Farrell, J., Miller, A. and Gaze, R., 2011, Geometallurgical Sampling and Resource Estimation for Magnetite Deposits: First AusIMM International Geometallurgy Conference (GeoMet), Brisbane, Australia, 5-7 September, Proceedings, p. 311-319.

Fettes, D. and Desmons, J., 2007, Metamorphic Rocks A Classification and Glossary of Terms: Cambridge, U.K, Cambridge University Press, 244 p.

Gaudin, A.M., 1939, Principles of Mineral Dressing: New York, USA, McGraw-Hill Companies, 554 p.

Gay, S.L., 2004, A liberation model for comminution based on probability theory: Minerals Engineering, v. 17, p. 525-534.

Geijer, P., 1930, Geology of the Gällivare Iron Ore field: Geological Survey of Sweden, v. Ca 22, p. 1-115.

Glacken, IM., Snowden, DV., 2001, Mineral Resource Estimation, *in* Mineral Resource and Ore Reserve Estimation – The AusIMM Guide to Good Practice, p. 189-198. The Australasian Institute of Mining and Metallurgy, Melbourne, Australia.

Gu, Y., 2003, Automated Scanning Electron Microscope Based Mineral Liberation analysis: Journal of Minerals & Materials Characterization & Engineering, v. 2, p. 33-41.

Haavisto, O. and Kaartinen, J., 2009, Multichannel reflectance spectral assaying of zinc and copper flotation slurries: International Journal of Mineral Processing, v. 93, p. 187-193.

Hunt, J., Berry, R., Bradshaw, D., Triffett, B. and Walters, S., 2012, Development of liberation/recovery domains: examples from the Prominent Hill IOCG deposit, Australia: Process Mineralogy'12, Cape Town, South Africa, 7-9 November, Proceedings, p. 1-16.

Hunt, J., Berry, R. and Bradshaw, D., 2011a, Characterising Liberation and Flotation Potential Using Image Analysis, Simulated Fragmentation and Small-Scale Flotation: The first AUSIMM international geometallurgy conference, Brisbane, Australia, 5-7 September, Proceedings, p. 331-333.

Hunt, J., Berry, R. and Bradshaw, D., 2011b, Characterising chalcopyrite liberation and flotation potential: Examples from an IOCG deposit: Minerals Engineering, v. 24, p. 1271-1276.

Hunt, J., Berry, R., Bonnici, N., Walters, S., Kamenetsky, M. and McMahon, C., 2009, From Drill Core to Processing - A Geometallurgical Approach to Mineralogy and Texure From Meso- to Micro-Scale: The Tenth Biennial SGA Meeting, Townsville, Australia, 17th-20th August, Proceedings, p. 685-687.

King, R.P. and Schneider, C.L., 1998, Mineral liberation and the batch communition equation: Minerals Engineering, v. 11, p. 1143-1160.

King, R.P., 1979, A model for the quantitative estimation of mineral liberation by grinding: International Journal of Mineral Processing, v. 6, p. 207-220.

Koch, P., 2013, Textural variants of iron ore from Malmberget: characterization, comminution and mineral liberation: Master thesis, Luleå, Sweden, Sustainable Process Engineering, Luleå University of Technology, 101p.

Lamberg, P. and Lund, C., 2012, Taking liberation information into a geometallurgical model-case study, Malmberget, Northern Sweden: Process Mineralogy'12 , Cape Town, South Africa, 7-9 November, Proceedings, p. 1-13.

Lamberg, P., 2011, Particles – the bridge between geology and metallurgy: Conference in mineral engineering, Luleå, Sweden, 8-9 February, Proceedings, p. 1-16.

Lamberg, P. and Vianna, S., 2007, A Technique for Tracking Multiphase Mineral Particles in Flotation Circuits: 7th Meeting of the Southern Hemisphere on the Mineral Technology, Ouro Preto, Brazil, Proceedings, p. 195-241.

Lamberg, P., Hautala, P., Sotka, S. and Saavalainen, S., 1997, Mineralogical balances by dissolution methodology: Short Course on 'Crystal Growth in Earth Sciences', S. Mamede de Infesta, Portugal, September 8-10, Proceedings, p. 1-29.

LKAB, 2011, Annual Report: Luleå, Sweden, Luleå Grafiska, 122 p.

Lund, C., Lamberg, P. and Lindberg, T., 2013, Practical way to quantify minerals from chemical assays at Malmberget iron ore operations – An important tool for the geometallurgical program: Minerals Engineering, v. 49, p. 7-16.

Lund, C., Lindberg, T. and Martinsson, O., 2010, Mineralogical-textural characterisation of different apatite-iron ore bodies, Malmberget deposit, Sweden, treated in a sorting process in laboratory scale: Process Mineralogy'10, Cape Town, South Africa, Proceedings, p. 1-9

Martinsson, O. and Virkkunen, R., 2004, Apatite Iron Ore in the Gällivare, Svappavaara, and Jukkasjärvi Areas: Society of Economics Geologists, Guidebooks Series, v. 33, p. 167-172.

Miller, J.D., Lin, C.L., Garcia, C. and Arias, H., 2003, Ultimate recovery in heap leaching operations as established from mineral exposure analysis by X-ray microtomography: International Journal of Mineral Processing, v. 72, p. 331-340.

Neumann, R. and Avelar, A.N., 2012, Refinement of the isomorphic substitutions in goethite and hematite by the Rietveld method, and relevance to bauxite characterisation and processing: Process Mineralogy '12, Vineyard Hotel, Cape Town, South Africa, 7-9 November, Proceedings, p. 1-10.

Niiranen, K. and Böhm, A., 2012, A systematic characterization of the ore body for mineral processing at Kiirunavaara iron ore mine operated by LKAB, Northern Sweden.: XXVI International Mineral Processing Congress (IMPC), New Delhi, India, Proceedings, p. 1039.

Paine, M., König, U. and Staples, E., 2011, Application of rapid X-ray diffraction (XRD) and cluster analysis to grade control of iron ores: Proceedings, 10th International Congress for Applied Mineralogy (ICAM), Trondheim, Norway, 1-5 August, Proceedings, p. 495-501.

Pérez-Barnuevo, L., Pirard, E. and Castroviejo, R., 2012, Automated textural analysis of the Kansanshi Copper ore: Process Mineralogy'12, Cape Town, South Africa, 7-9 November, Proceedings, p. 1-16.

Pirard, E., Bernhardt, HJ., Catalina, JC., Brea, C., Segundo, F., Castroviejo, R., 2008, From spectrophotometry to multispectral imaging of ore minerals in visible and near infrared (VNIR) microscopy. Proceedings, 9th International Congress for Applied Mineralogy (ICAM 2008), 8-10 september, Brisbane, Australia.

Pitard, F.F., 1989, Pierre Gy's sampling theory and sampling practice Vol. 2, Sampling theory and sampling practice: Boca raton fl, US, CRC Press, 247 p.

Spray, A., 1969, Metamorphic textures, Pergamon Press, 350 p

Stamboliadis, E.T., 2008, The evolution of a mineral liberation model by the repetition of a simple random breakage pattern: Minerals Engineering, v. 21, p. 213-223.

Suazo, C.J., Kracht, W. and Alruiz, O.M., 2010, Geometallurgical modelling of the Collahuasi flotation circuit: Minerals Engineering, v. 23, p. 137-142.

Sutherland, D.N. and Gottlieb, P., 1991, Application of automated quantitative mineralogy in mineral processing: Minerals Engineering, v. 4, p. 753-762.

Vogel, L. and Peukert, W., 2003, Breakage behaviour of different materials—construction of a mastercurve for the breakage probability: Powder Technology, v. 129, p. 101-110.

Weller, K.R., Morrell, S. and Gottlieb, P., 1996, Use of grinding and liberation models to simulate tower mill circuit performance in a lead/zinc concentrator to increase flotation recovery: International Journal of Mineral Processing, v. 44–45, p. 683-702.